

# Stochastic Information Geometry: Characterization of Fréchet Means of Gaussian Fields in Poisson Networks

Gourab Ghatak

**Abstract**—We develop a unified framework for distributed inference, semantic communication, and exploration in spatial networks by integrating stochastic geometry with information geometry - a direction that has not been explored in prior literature. Specifically, we study the problem of estimating and aggregating a field of Gaussian distributions indexed by a spatial Poisson point process (PPP), under both the Fisher–Rao and 2-Wasserstein geometries. We derive non-asymptotic concentration bounds and Palm deviations for the empirical Fréchet mean, thereby quantifying the geometric uncertainty induced by spatial randomness. Building on these results, we demonstrate applications to wireless sensor networks, where our framework provides geometry-aware aggregation methods that downweight unreliable sensors and rigorously characterize estimation error under random deployment. Further, we extend our theory to semantic communications, proposing compression protocols that guarantee semantic fidelity via distortion bounds on Fréchet means under PPP sampling. Finally, we introduce the Fréchet–UCB algorithm for multi-armed bandit problems with heteroscedastic Gaussian rewards. This algorithm combines upper confidence bounds with a geometry-aware penalty reflecting deviation from the evolving Fréchet mean, and we derive regret bounds that exploit geometric structure. Simulations validate the theoretical predictions across wireless sensor networks, semantic compression tasks, and bandit environments, highlighting scalability, robustness, and improved decision-making. Our results provide a principled mathematical foundation for geometry-aware inference, semantic communication, and exploration in distributed systems with statistical heterogeneity.

**Index Terms**—Information geometry, stochastic geometry, Fréchet mean, Gaussian manifold, wireless sensor networks, Wasserstein distance, Fisher–Rao metric, distributional bandits.

## I. INTRODUCTION

In many modern applications of distributed sensing, learning, and decision-making, such as environmental monitoring, robotics, and wireless communications, agents operate in spatially uncertain environments [1]. These agents often make noisy, partial observations of underlying phenomena and build local probabilistic models to represent their beliefs. A key challenge lies in how to combine such probabilistic representations across a randomly deployed network to arrive at a consistent, global inference or decision-making. More importantly, a network designer may be interested in studying how does the combined inference vary across different realizations of such networks. A natural and powerful way to model such agent beliefs is via the geometry of probability distributions. In particular, the space of Gaussian distributions admits rich geometric structures, notably the Fisher–Rao and Wasserstein geometries [2]–[4]. These geometries endow the space of distributions with a Riemannian manifold structure,

enabling meaningful notions of distance, averaging, and optimization [5].

Simultaneously, spatial randomness such as that arising from sensor drops, mobility, or fading environments can be modeled using the tools of stochastic geometry, particularly Poisson point processes (PPPs) [6]. The statistical regularity of PPPs allows analytical tractability while capturing essential deployment uncertainty. In this paper, we bridge these two powerful frameworks by studying the information geometry of spatial Gaussian fields over PPPs. Specifically, we consider a point process of agents in the Euclidean plane  $\mathbb{R}^2$ , where each agent samples its local environment and models its belief as a Gaussian distribution,  $\mathcal{N}(\mu_x, \Sigma_x)$ , leading to a random field  $\{p_x\}_{x \in \Phi}$ , where  $\Phi \subset \mathbb{R}^2$  is a realization of a PPP. The key consideration is the fact that the geometry of the locations of these agents in  $\mathbb{R}^2$  may vary from the geometry of their corresponding distributions in the information space. Our goal is to compute and analyze the *Fréchet mean* (also called the geometric barycenter) of these distributions, under both the Fisher–Rao and Wasserstein metrics (e.g., see [7]). This fusion enables a principled approach to aggregating beliefs in sensor networks using geometry-aware averages, quantifying spatial uncertainty using Palm calculus, characterizing convergence using empirical process theory on manifolds, designing novel algorithms for distributional bandits that respect the underlying geometry. The integration of information geometry, stochastic geometry, and distributed statistical inference has potential applications across multiple domains, including signal processing, machine learning, and network science. However, to the best of our knowledge such a characterization of stochastic information geometry has not been done in prior work.

### A. Related Works

Information geometry provides a differential geometric framework to study statistical models by treating families of probability distributions as Riemannian manifolds. The foundational work of Amari and Nagaoka introduced the Fisher–Rao metric and its implications for the statistical manifold structure of exponential families, including the Gaussian family [8]. Subsequent research has characterized geodesics, curvature, and the Fréchet mean under this geometry [9], [10]. In particular, the manifold of Gaussian distributions has been extensively studied due to its closed-form expressions in special cases and tractable geometric properties. Parallel to this, the Wasserstein geometry arising from optimal transport theory has been used to define meaningful distances and averages over probability measures with finite second moments. The Wasserstein metric, especially the 2-Wasserstein distance, has

been shown to induce a Riemannian structure over Gaussian distributions [11], [12], leading to applications in distributional learning and generative modeling [13]. The distribution of the Fréchet mean with the Wasserstein metric was thoroughly studied in the thesis by Zemel [14]. In this work, we extend the same to locations based on stochastic point processes.

On the other hand, stochastic geometry, particularly the theory of PPPs, offers analytical tools for modeling spatial randomness in wireless networks, sensor deployments, and robotics. Classical references such as [15] and [16] provide rigorous formulations for spatial expectations, Palm calculus, and empirical process approximations. Campbell's theorem and Palm distributions have been used to characterize average behavior and typical deviations in spatial fields, but rarely in conjunction with geometric structures on statistical manifolds.

The idea of combining information geometry with spatial randomness remains relatively underexplored. Previous attempts to model distributed probabilistic inference over networks have largely focused on Euclidean spaces or scalar-valued summaries. For instance, consensus and distributed averaging algorithms assume additive noise and operate in vector spaces [17], neglecting the curvature and metric structure of distributional models. Recent advances in distributed machine learning have proposed Wasserstein barycenter computations in federated setups [18], but without incorporating spatial point process modeling. A closely related body of literature addresses aggregation over the manifold of covariance matrices, often using the affine-invariant Riemannian metric [19]. These approaches provide insights into averaging and interpolation on symmetric positive definite (SPD) manifolds, yet they typically assume fixed spatial topologies or deterministic node placements. In contrast, our work introduces a fully probabilistic model where Gaussian distributions arise from i.i.d. sampling over spatially random agents, and their aggregation is analyzed through the lens of both Fisher–Rao and Wasserstein geometries.

In the context of wireless sensor networks (WSNs), several works have considered probabilistic fusion of information from spatially deployed nodes [20]. However, traditional models typically employ scalar belief representations or Gaussian mixtures without explicitly modeling the underlying geometry of distributions or the randomness in spatial configuration. Our approach addresses this gap by incorporating geometric averaging over a random spatial field of distributions and rigorously analyzing its convergence using tools from stochastic geometry. Finally, multi-armed bandit (MAB) problems with structured or nonparametric reward models have drawn attention in recent years [21], [22]. The idea of using distributional rather than scalar rewards has led to the development of distributional bandits [23], yet most such works rely on empirical divergences (e.g., KL divergence, total variation) rather than Riemannian geometric notions. The *Fréchet-UCB* algorithm proposed in this paper differs fundamentally by integrating both the geometry of distributions and the spatial structure of the arms via PPP modeling. Moreover, our regret analysis accounts for the metric-induced neighborhood of the optimal arm, introducing novel bounds that incorporate spatial coverage and curvature.

## B. Main Contributions

This paper proposes a novel synthesis of information geometry and stochastic geometry to address distributed inference and decision-making in spatially random networks. The originality of our work lies in unifying the Riemannian structure of probability distributions (e.g., under Fisher–Rao and 2-Wasserstein metrics) with spatially distributed statistical fields modeled via PPP. The key technical contributions are as follows:

1) We formulate and rigorously analyze the problem of computing the Fréchet mean of a spatial field of Gaussian distributions  $\{p_x\}_{x \in \Phi}$ , where  $\Phi$  is a realization of a homogeneous or nonhomogeneous PPP. The distributions are endowed with either the Fisher–Rao or Wasserstein geometry, yielding a non-Euclidean aggregation framework. Using tools from Palm theory, Campbell's theorem, and empirical process theory on manifolds, we derive precise expressions for the expected Fréchet mean, its concentration, and Palm deviations.

2) We analyze the distribution of the empirical Fréchet mean conditioned on a realization of the PPP, leading to the *meta-distribution* of geometric inference. This framework allows us to quantify semantic distortion in compressed representations of distributional fields and derive bounds for geometry-preserving sub-sampling in semantic communications.

3) Applications to wireless sensor networks: We apply the developed framework to wireless sensor networks, showing how geometry-aware aggregation improves robustness against unreliable sensors, and we provide concentration-based guidelines for deployment size to achieve a desired estimation accuracy. Simulation results confirm the advantages of Fréchet aggregation compared to Euclidean averaging.

4) Applications to semantic communications: We extend our results to semantic compression over spatial networks, proposing protocols for subsampling sensor fields while preserving semantic fidelity. We derive explicit conditions on sparse PPP intensities to guarantee bounded semantic distortion, yielding design principles for communication-efficient, geometry-aware protocols.

5) Next, we introduce the *Fréchet-UCB* algorithm for bandit problems with heteroscedastic Gaussian rewards and spatially embedded arms. The algorithm selects arms by combining upper confidence bounds with a geometric penalty relative to the evolving Fréchet mean. We derive a new regret bound that accounts for geodesic neighborhoods, suboptimality gaps, and the spatial distribution of arms, distinguishing between local and global exploration regimes. We show that such geometric considerations may lead to better decision making under uncertainty especially in case of randomly located large-scale distributions (i.e., large number of arms with stochastic parameters).

6) We demonstrate that the developed framework provides a common mathematical foundation for aggregation, uncertainty quantification, and regret-optimal decision-making over spatial statistical manifolds. The theoretical predictions are validated by simulations involving wireless sensor networks and multi-armed bandits, confirming scalability and robustness.

To our knowledge, this is the first work to rigorously connect spatial stochastic processes with Riemannian information

Table I: Summary of Notations

Symbol	Description
$\Phi$	Spatial PPP
$p_x$	Gaussian distribution at location $x$
$N(\mu_x, \Sigma_x)$	Gaussian with mean $\mu_x$ and covariance $\Sigma_x$
$\mathcal{M}$	Manifold of Gaussians
$d(p_1, p_2)$	Geodesic distance between distributions
$\bar{p}$	Global Fréchet mean of the field
$\hat{p}_R$	Empirical Fréchet mean over $B_R$
$\mu_x, \Sigma_x$	Mean and covariance of $p_x$
$\Gamma$	Covariance of the local means $\mu_x$
$\Delta_{\text{Palm}}$	Expected local deviation under Palm
$\mathcal{N}_\varepsilon(\hat{p}_t)$	Geodesic neighborhood of the Fréchet mean
$T$	Time horizon for bandit problems
$K$	Number of arms
$\mu_k, \sigma_k^2$	Mean and variance of arm $k$
$\hat{\mu}_{\text{Fr}}(t)$	Precision-weighted Fréchet mean at time $t$
$\text{Regret}(T)$	Cumulative expected regret up to time $T$

geometry to yield convergence results, performance bounds, and algorithmic design principles.

### C. Organization and Notations

Section II reviews the Fisher–Rao and 2-Wasserstein geometry of Gaussian distributions. Section III introduces the spatial marked Poisson model and formulates the inference objectives. Section IV derives concentration bounds for the empirical Fréchet mean using stochastic geometry. Section V studies the meta-distribution of the Fréchet mean under conditioning. Section VI applies the framework to distributed wireless sensing, while Section VII extends it to semantic compression in spatial networks. Section VIII introduces the Fréchet–UCB algorithm and analyzes its regret. Finally, Section IX concludes the paper. Throughout, we use the notation summarized in Table I.

**Note:** In case of ambiguity between Fréchet *mean* and the *mean* of the Fréchet mean, we refer to the later as the *mean of the Fréchet barycenter*.

## II. GEOMETRY OF GAUSSIANS: KEY DEFINITIONS AND METRICS

Information geometry provides a differential geometric framework for studying stochastic models, where the probability distributions are treated as points on a Riemannian manifold. For parametric families of distributions, particularly exponential families, this geometry is induced by the Fisher–Rao metric, which we first develop below. We follow this by a discussion based on the Wasserstein metric.

### A. Fisher–Rao Metric

Let  $\mathcal{N}(\mu, \Sigma)$  denote the multivariate Gaussian distribution with mean  $\mu \in \mathbb{R}^d$  and covariance matrix  $\Sigma \in \mathbb{S}_{++}^d$ , the space of  $d \times d$  SPD matrices. The family of multivariate Gaussians forms a smooth manifold  $\mathcal{M} = \{\mathcal{N}(\mu, \Sigma) \mid \mu \in \mathbb{R}^d, \Sigma \in \mathbb{S}_{++}^d\}$ , with  $(\mu, \Sigma)$  being the coordinates of this manifold. In

the first setting, we assume that the geometry of  $\mathcal{M}$  is endowed with the Fisher–Rao metric, which induces a Riemannian structure on this space. In general, for a probability density function  $p(x; \theta)$ , parameterized on  $\theta$ , the Fisher information matrix is

$$I(\theta) = \mathbb{E}_{x \sim p(\cdot; \theta)} [\nabla_\theta \log p(x; \theta) \nabla_\theta \log p(x; \theta)^\top]. \quad (1)$$

For the multivariate Gaussian  $p(x; \mu, \Sigma)$ , where  $\theta = (\mu, \Sigma)$ , the Fisher–Rao metric has the structure  $g_{\mu\mu} = \Sigma^{-1}$ , and  $g_{\Sigma\Sigma} = \frac{1}{2}\Sigma^{-1} \otimes \Sigma^{-1}$ , where  $\otimes$  denotes the Kronecker product [24]. Hence, the squared line element (metric) is

$$ds^2 = d\mu^\top \Sigma^{-1} d\mu + \frac{1}{2} \text{Tr}(\Sigma^{-1} d\Sigma \Sigma^{-1} d\Sigma). \quad (2)$$

This metric is invariant under affine transformations and reflects the statistical structure of the Gaussian family. Accordingly, let  $p_1 = \mathcal{N}(\mu_1, \Sigma_1)$  and  $p_2 = \mathcal{N}(\mu_2, \Sigma_2)$ . The geodesic distance  $d(p_1, p_2)$  under the Fisher–Rao metric is not available in closed form for general  $(\mu, \Sigma)$ , but several special cases are tractable. For example, if the covariance is the same, i.e.,  $\Sigma_1 = \Sigma_2 = \Sigma$ , we have  $d^2(p_1, p_2) = (\mu_1 - \mu_2)^\top \Sigma^{-1} (\mu_1 - \mu_2)$ , i.e., the Mahalanobis distance (this will be exploited later, e.g., in Theorem 1). If the means are the same, i.e.,  $\mu_1 = \mu_2$  but with different covariances, then  $d^2(p_1, p_2) = \frac{1}{2} \sum_{i=1}^d \log^2 \lambda_i$ , where  $\lambda_1, \dots, \lambda_d$  are the eigenvalues of  $\Sigma_1^{-1/2} \Sigma_2 \Sigma_1^{-1/2}$ . For further special cases and discussion, we refer the reader to [25].

**Definition 1.** The Fréchet mean  $\bar{p} \in \mathcal{M}$  of a collection  $\{p_i\}$  minimizes the sum of squared geodesic distances  $\bar{p} = \arg \min_{p \in \mathcal{M}} \sum_i d^2(p_i, p)$ .

This is typically computed via iterative Riemannian gradient descent algorithms [26]. As a particular case, we make the following remark.

**Remark 1.** On  $\mathbb{S}_{++}^d$ , an alternative and widely used metric is the affine-invariant Riemannian metric  $d_R(\Sigma_1, \Sigma_2) = \left\| \log \left( \Sigma_1^{-1/2} \Sigma_2 \Sigma_1^{-1/2} \right) \right\|_F$ , which coincides with the Fisher–Rao distance when the mean is fixed.

**Definition 2.** Given a set of Gaussians  $\{\mathcal{N}(\mu_i, \Sigma_i)\}_{i=1}^n$ , the Fréchet mean under the Fisher–Rao metric is  $\bar{p} = \mathcal{N}(\bar{\mu}, \bar{\Sigma}) = \arg \min_{(\mu, \Sigma)} \sum_{i=1}^n d^2(\mathcal{N}(\mu_i, \Sigma_i), \mathcal{N}(\mu, \Sigma))$ .

**Corollary 1.** If  $\Sigma_i = \Sigma$ , then  $\bar{\mu} = \frac{1}{n} \sum_{i=1}^n \mu_i$ ,  $\bar{\Sigma} = \Sigma$ . On the other hand, if  $\mu_i = \mu$  (fixed mean), then  $\bar{\Sigma}$  is the Riemannian barycenter of  $\{\Sigma_i\}$  under the metric  $d_R = \bar{\Sigma} = \arg \min_{\Sigma} \sum_i d_R^2(\Sigma_i, \Sigma)$ .

### B. Wasserstein Metric

The Wasserstein geometry arises from the theory of optimal transport, where the 2-Wasserstein distance  $W_2(\cdot, \cdot)$  defines a Riemannian structure on the space of probability measures with finite second moments, denoted  $\mathcal{P}_2(\mathbb{R}^d)$ . This geometry provides an alternative to the Fisher–Rao geometry and has gained prominence in applications involving distributional

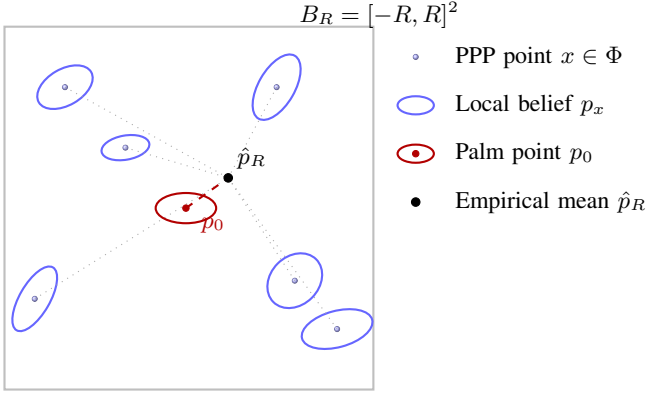


Fig. 1. Illustration of Gaussian beliefs  $\{p_x\}_{x \in \Phi}$  over a spatial PPP confined to a bounded region  $B_R = [-R, R]^2$ . Each small blue dot represents a point  $x \in \Phi$ , and the blue ellipse centered at  $x$  encodes the corresponding local Gaussian belief  $p_x = \mathcal{N}(\mu_x, \Sigma_x)$ . The red ellipse at the origin denotes the Palm point  $p_0$ , and the black dot represents the empirical Fréchet mean  $\hat{p}_R$  computed over  $\Phi \cap B_R$ . Dotted gray lines connect each local distribution  $p_x$  to the empirical mean  $\hat{p}_R$ , representing geodesic deviations under the Fisher–Rao or Wasserstein geometry. The dashed red line highlights the deviation between the Palm point  $p_0$  and  $\hat{p}_R$ , which plays a key role in quantifying semantic dispersion.

averaging and generative modeling. The squared 2-Wasserstein distance between  $p_1 = \mathcal{N}(\mu_1, \Sigma_1)$  and  $p_2 = \mathcal{N}(\mu_2, \Sigma_2)$  is

$$W_2^2(p_1, p_2) = \|\mu_1 - \mu_2\|_2^2 + \text{Tr} \left( \Sigma_1 + \Sigma_2 - 2 \left( \Sigma_1^{1/2} \Sigma_2 \Sigma_1^{1/2} \right)^{1/2} \right). \quad (3)$$

The first term measures the Euclidean distance between the means, and the second term captures the geometric discrepancy between the covariances. Under the 2-Wasserstein metric, the space of Gaussians  $\mathcal{G} = \{\mathcal{N}(\mu, \Sigma)\}$  forms a Riemannian manifold  $\mathcal{M}_W$ .

**Definition 3.** Given a set of Gaussians  $\{\mathcal{N}(\mu_i, \Sigma_i)\}_{i=1}^n$ , the Wasserstein Fréchet mean or the Wasserstein barycenter is defined as the minimizer of the average squared Wasserstein distance. Mathematically,

$$\bar{p}_W = \arg \min_{p \in \mathcal{G}} \sum_{i=1}^n W_2^2(p, p_i). \quad (4)$$

The mean component is simply  $\bar{\mu} = \frac{1}{n} \sum_{i=1}^n \mu_i$ , while the covariance component  $\bar{\Sigma}$  solves the following:

$$\bar{\Sigma} = \arg \min_{\Sigma \in \mathbb{S}_{++}^d} \sum_{i=1}^n \text{Tr} \left( \Sigma + \Sigma_i - 2 \left( \Sigma^{1/2} \Sigma_i \Sigma^{1/2} \right)^{1/2} \right). \quad (5)$$

This problem is convex and can be solved using fixed-point iteration or manifold optimization techniques [27]. Of course, for the one dimensional Gaussian,  $\bar{\Sigma} := \bar{\sigma} = \frac{1}{n} \sum_{i=1}^n \sigma_i$ .

### III. SYSTEM MODEL AND OBJECTIVES

We consider a distributed statistical inference problem, where spatially dispersed agents (e.g., wireless sensors) are randomly deployed over a two-dimensional Euclidean plane. Each agent locally observes data and models it using a Gaussian distribution. The spatial randomness in the deployment is modeled via a homogeneous PPP. Our objective is to characterize the global geometric average, i.e., Fréchet mean or Wasserstein barycenter, of these Gaussian distributions under Fisher–Rao and Wasserstein geometry, respectively.

#### A. Marked Spatial Poisson Model of Information Sources

We model the spatial layout of information sources as a realization  $\Phi = \{x_i\}_{i \in \mathbb{N}} \subset \mathbb{R}^2$  of a PPP with intensity measure  $\Lambda(dx) = \lambda(x) dx$ , where  $\lambda(x)$  is a locally integrable intensity function. Each spatial location  $x \in \Phi$  is associated with a probability distribution  $p_x$ , capturing the local uncertainty or belief of the agent at  $x$  about an underlying phenomenon. Specifically, we assume that  $p_x = \mathcal{N}(\mu_x, \Sigma_x)$  is a location-dependent Gaussian distribution mark, where both the mean  $\mu_x \in \mathbb{R}^d$  and covariance  $\Sigma_x \in \mathbb{S}_{++}^d$  may vary arbitrarily across space. That is, the pair  $(\mu_x, \Sigma_x)$  is a measurable function of location, possibly reflecting local sensing quality, environmental noise, or prior knowledge. We denote by  $\Gamma$  the variance of  $\mu_x$  across agents.

This setup defines a *distribution marked point process* [6], where each point  $x \in \Phi$  carries a statistical mark  $p_x$ , which is not a random variable but a distribution. The distributions  $\{p_x\}$  are spatially coupled through their deterministic or stochastic dependence on  $x$ . Let  $d(\cdot, \cdot)$  denote a divergence or geodesic distance on the space of probability distributions (e.g., Fisher–Rao or Wasserstein distance). Given a bounded spatial domain  $B \subset \mathbb{R}^2$ , we define the empirical Fréchet mean  $\hat{p}_B$  as  $\hat{p}_B = \arg \min_{q \in \mathcal{G}} \sum_{x \in \Phi \cap B} d^2(p_x, q)$ , where  $\mathcal{G}$  is the manifold of Gaussian distributions. As  $|B| \rightarrow \infty$ , this empirical mean approximates the expected geodesic barycenter

$$\bar{p} = \arg \min_{q \in \mathcal{G}} \lambda \int_{\mathbb{R}^2} \mathbb{E}_{p_x} [d^2(p_x, q)] dx, \quad (6)$$

where the expectation may be interpreted under any stochastic model for  $\mu_x$  and  $\Sigma_x$  if they are random fields. This formulation treats the spatial distribution of beliefs as an information source ensemble, and the goal is to aggregate distributed beliefs into a global, geometry-respecting representation. To analyze its asymptotic behavior as  $|B| \rightarrow \infty$ , we invoke tools from stochastic geometry. Specifically, by Campbell’s theorem, the expectation of a sum over a marked PPP can be expressed as a spatial integral over the product of the intensity and the expected mark functional [6]

$$\mathbb{E} \left[ \sum_{x \in \Phi} f(x, p_x) \right] = \int_{\mathbb{R}^2} \lambda(x) \mathbb{E}[f(x, p_x)] dx. \quad (7)$$

Applying this to the metric functional  $f(x, p_x) = d^2(p_x, q)$  yields the limiting Fréchet mean,  $\bar{p} = \arg \min_{q \in \mathcal{G}} \int_{\mathbb{R}^2} \lambda(x) \mathbb{E}[d^2(p_x, q)] dx$ , which represents the asymptotic geometric barycenter of the spatially varying information sources.

Furthermore, to understand the variability of individual agents' beliefs relative to the global mean, we appeal to Palm theory. The Palm distribution of  $\Phi$  conditions on the existence of a point at a specific location, say  $0 \in \mathbb{R}^2$ . The expected squared distance between the typical mark  $p_0$  and the global mean  $\bar{p}$  under the Palm distribution is  $\Delta_{\text{Palm}} := \mathbb{E}[d^2(p_0, \bar{p}) \mid 0 \in \Phi]$ , which quantifies the expected local deviation of a typical agent from the global belief. This can be interpreted as a spatially averaged divergence and serves as a measure of geometric dispersion in the belief field. In information-theoretic terms, it reflects the redundancy or heterogeneity in the distributed information representation. This marked point process formulation allows the incorporation of spatial non-stationarity and heterogeneity in belief formation, and enables rigorous analysis using integral geometry and empirical process theory on manifolds.

This setup is illustrated in Fig. 1, where we visualize the distribution-valued marked point process and the empirical Fréchet mean over a bounded observation window.

### B. Objectives

The central questions we aim to address are as follows: (i) what is the structure of the global Fréchet mean  $\bar{p}$  of a field of Gaussian distributions indexed by a spatial PPP, under different choices of metrics such as the Fisher–Rao and 2-Wasserstein geometries? (ii) how does the geometry of the mean depend on the statistical properties of the field, particularly the spatial distribution and second-order statistics of the local means  $\mu_x$  and covariances  $\Sigma_x$ ? (iii) can we derive rigorous concentration bounds and characterize the fluctuation behavior of the empirical Fréchet mean over growing spatial domains using tools from stochastic geometry, including Campbell's theorem and empirical process theory on manifolds? (iv) what is the expected local deviation of a typical node from the global mean, as quantified via Palm calculus, and how does this deviation reflect the semantic dispersion and heterogeneity of the distributed belief field?

## IV. STATISTICS OF THE RANDOM FRÉCHET MEAN

In this section, we derive rigorous theoretical results concerning the structure and behavior of the Fréchet mean  $\bar{p}$  of Gaussian distributions  $\{p_x\}_{x \in \Phi}$  associated with  $\Phi$ .

**Theorem 1** (Fréchet mean under Fisher–Rao metric with location-dependent means). *The asymptotic Fréchet mean  $\bar{p} = \mathcal{N}(\bar{\mu}, \bar{\Sigma})$  under the Fisher–Rao metric is given by*

$$\bar{\mu} = \frac{1}{\Lambda(B)} \int_B \mu_x \lambda(x) dx, \quad \text{where } \Lambda(B) := \int_B \lambda(x) dx,$$

for any bounded domain  $B \subset \mathbb{R}^2$ . Moreover, the expected squared Fisher–Rao distance between a typical distribution  $p_x$  and the global mean  $\bar{p}$  is

$$\mathbb{E}[d^2(p_x, \bar{p})] = \frac{1}{\Lambda(B)} \int_B (\mu_x - \bar{\mu})^\top \Sigma^{-1} (\mu_x - \bar{\mu}) \lambda(x) dx.$$

*Proof.* The proof follows trivially by observing that under the Fisher–Rao metric with fixed covariance  $\Sigma$ , the geodesic

squared distance between two Gaussian distributions  $p_x = \mathcal{N}(\mu_x, \Sigma)$  and  $q = \mathcal{N}(\mu_q, \Sigma)$  reduces to the Mahalanobis distance,  $d^2(p_x, q) = (\mu_x - \mu_q)^\top \Sigma^{-1} (\mu_x - \mu_q)$  [28]. The Fréchet mean  $\bar{p} = \mathcal{N}(\bar{\mu}, \Sigma)$  minimizes the expected squared distance over space  $\bar{\mu} = \arg \min_{\mu_q \in \mathbb{R}^d} \int_B (\mu_x - \mu_q)^\top \Sigma^{-1} (\mu_x - \mu_q) \lambda(x) dx$ . This is a strictly convex quadratic minimization problem whose unique minimizer is the weighted spatial average  $\bar{\mu} = \frac{1}{\Lambda(B)} \int_B \mu_x \lambda(x) dx$ . Substituting this into the expected squared distance expression yields:  $\mathbb{E}[d^2(p_x, \bar{p})] = \frac{1}{\Lambda(B)} \int_B (\mu_x - \bar{\mu})^\top \Sigma^{-1} (\mu_x - \bar{\mu}) \lambda(x) dx$ , completing the proof.  $\square$

**Theorem 2** (Fréchet mean under 2-Wasserstein metric with location-dependent means). *Let  $\{p_x\}_{x \in B}$  be Gaussians  $p_x = \mathcal{N}(\mu_x, \Sigma_x)$  indexed by  $x \in B \subset \mathbb{R}^2$  with intensity density  $\lambda(x)$  and  $\Lambda(B) := \int_B \lambda(x) dx$ . The 2-Wasserstein Fréchet mean  $\bar{p}_W = \mathcal{N}(\bar{\mu}, \bar{\Sigma})$  minimizes the spatial functional  $\bar{p}_W = \arg \min_{p \in \mathcal{G}} \int_B \lambda(x) W_2^2(p, p_x) dx$ , and its mean component is the weighted spatial average  $\bar{\mu} = \frac{1}{\Lambda(B)} \int_B \mu_x \lambda(x) dx$ . The covariance  $\bar{\Sigma}$  is the unique solution in  $S_d^{++}$  of the convex variational problem*

$$\bar{\Sigma} = \arg \min_{\Sigma \in S_d^{++}} \int_B \lambda(x) \text{Tr} \left( \Sigma + \Sigma_x - 2(\Sigma^{1/2} \Sigma_x \Sigma^{1/2})^{1/2} \right) dx.$$

In particular, when  $\Sigma_x \equiv \Sigma$  (common covariance),  $\bar{\Sigma} = \Sigma$  and the expected squared 2-Wasserstein distance between a typical  $p_x$  and  $\bar{p}_W$  reduces to

$$\mathbb{E}[W_2^2(p_x, \bar{p}_W)] = \frac{1}{\Lambda(B)} \int_B \|\mu_x - \bar{\mu}\|^2 \lambda(x) dx.$$

*Proof.* Recall that the squared 2-Wasserstein distance between two Gaussian distributions  $\mathcal{N}(\mu, \Sigma)$  and  $\mathcal{N}(\mu_x, \Sigma_x)$  is

$$\begin{aligned} W_2^2(\mathcal{N}(\mu, \Sigma), \mathcal{N}(\mu_x, \Sigma_x)) \\ = \|\mu - \mu_x\|^2 + \text{Tr} \left( \Sigma + \Sigma_x - 2(\Sigma^{1/2} \Sigma_x \Sigma^{1/2})^{1/2} \right). \end{aligned} \quad (8)$$

The Fréchet mean  $\bar{p}_W = \mathcal{N}(\bar{\mu}, \bar{\Sigma})$  minimizes the functional

$$J(\mu, \Sigma) = \int_B \lambda(x) W_2^2(\mathcal{N}(\mu, \Sigma), \mathcal{N}(\mu_x, \Sigma_x)) dx. \quad (9)$$

Substituting (8) into  $J(\mu, \Sigma)$ , we see that

$$\begin{aligned} J(\mu, \Sigma) = & \underbrace{\int_B \lambda(x) \|\mu - \mu_x\|^2 dx}_{J_1(\mu)} + \\ & \underbrace{\int_B \lambda(x) \text{Tr} \left( \Sigma + \Sigma_x - 2(\Sigma^{1/2} \Sigma_x \Sigma^{1/2})^{1/2} \right) dx}_{J_2(\Sigma)}. \end{aligned} \quad (10)$$

The two terms  $J_1(\mu)$  and  $J_2(\Sigma)$  depend on  $\mu$  and  $\Sigma$  separately. The functional  $J_1(\mu)$  is strictly convex in  $\mu$ ; differentiating and setting the gradient to zero yields

$$\bar{\mu} = \frac{1}{\Lambda(B)} \int_B \mu_x \lambda(x) dx, \quad (11)$$

where  $\Lambda(B) = \int_B \lambda(x) dx$ . The functional  $J_2(\Sigma)$  is convex over the space  $S_d^{++}$ . Hence it admits a unique minimizer  $\bar{\Sigma}$

satisfying

$$\bar{\Sigma} = \arg \min_{\Sigma \in S_d^{++}} \int_B \lambda(x) \operatorname{Tr} \left( \Sigma + \Sigma_x - 2(\Sigma^{1/2} \Sigma_x \Sigma^{1/2})^{1/2} \right) dx. \quad (12)$$

In the special case where  $\Sigma_x \equiv \Sigma$  for all  $x \in B$ , the integrand in  $J_2(\Sigma)$  vanishes when  $\Sigma = \Sigma_x$ , so  $\bar{\Sigma} = \Sigma$  and  $J_2(\Sigma)$  is minimized trivially.

When  $\Sigma_x \equiv \Sigma$ , substituting  $(\bar{\mu}, \bar{\Sigma})$  into (8) yields

$$\mathbb{E}[W_2^2(p_x, \bar{p}_W)] = \frac{1}{\Lambda(B)} \int_B \|\mu_x - \bar{\mu}\|^2 \lambda(x) dx, \quad (13)$$

completing the proof.  $\square$

**Remark 2.** Theorem 2 is the direct analogue of Theorem 1 for the 2-Wasserstein metric. In both cases, the mean component of the Fréchet barycenter is the spatially weighted average of the local means  $\mu_x$ . The difference lies in the treatment of the covariance - under the Fisher-Rao metric (Theorem 1), the barycenter covariance has a closed-form expression involving the inverse of the averaged precision matrices, whereas in the Wasserstein case it is obtained by solving a convex matrix minimization problem involving matrix geometric means. In the special case of identical covariances, both metrics yield  $\bar{\Sigma} = \Sigma$  and the optimization reduces to computing  $\bar{\mu}$ .

**Corollary 2.** Suppose the assumptions of Theorem 1 hold, and in addition, the local distributions  $p_x = \mathcal{N}(\mu_x, \Sigma)$  are independent and identically distributed across all  $x \in \Phi$ , with  $\mu_x \sim \mathcal{N}(\bar{\mu}, \Gamma)$ , and  $\Sigma$  fixed. Then the population Fréchet mean is  $\bar{p} = \mathcal{N}(\bar{\mu}, \Sigma)$ , and the expected squared Fisher-Rao distance from a typical agent to the mean simplifies to

$$\mathbb{E}[d^2(p_x, \bar{p})] = \operatorname{Tr}(\Sigma^{-1} \Gamma).$$

Similarly, the expected squared Wasserstein distance to the mean is

$$\mathbb{E}[W_2^2(p_x, \bar{p})] = \operatorname{Tr}(\Gamma).$$

*Proof.* Under the i.i.d. assumption, the mean vectors  $\mu_x$  are drawn from a common distribution with mean  $\bar{\mu}$  and covariance  $\Gamma$ . By Theorem 1, the Fisher-Rao distance simplifies to the Mahalanobis form due to fixed  $\Sigma$ ,  $\mathbb{E}[d^2(p_x, \bar{p})] = \mathbb{E}[(\mu_x - \bar{\mu})^\top \Sigma^{-1} (\mu_x - \bar{\mu})] = \operatorname{Tr}(\Sigma^{-1} \Gamma)$ , using the identity  $\mathbb{E}[X X^\top] = \operatorname{Cov}(X)$  when  $\mathbb{E}[X] = 0$ . This matches the special case computed earlier, and the spatial integration in Theorem 1 collapses due to stationarity and independence of the marks from  $x$ . Furthermore, since the Wasserstein distance reduces to squared Euclidean norm between means when covariances are fixed,  $\mathbb{E}[W_2^2(p_x, \bar{p})] = \mathbb{E}[\|\mu_x - \bar{\mu}\|^2] = \operatorname{Tr}(\Gamma)$ , by standard properties of the multivariate normal distribution [29].  $\square$

#### A. Concentration of Empirical Fréchet Mean

First, for a particular point of the PPP, a simple application of Hanson-Wright inequality [30] and Cantelli's inequality [31] gives the following result.

**Corollary 3.** The squared Fisher-Rao distance  $X := d^2(p_x, \bar{p}) = (\mu_x - \bar{\mu})^\top \Sigma^{-1} (\mu_x - \bar{\mu})$  satisfies the concentration

inequality

$$\mathbb{P}(X \geq \operatorname{Tr}(\Sigma^{-1} \Gamma) + t) \leq \exp \left( -\frac{t^2}{8 \cdot \operatorname{Tr}[(\Sigma^{-1} \Gamma)^2]} \right), \quad (14)$$

and the one-sided Cantelli-type bound

$$\mathbb{P}(X \geq \operatorname{Tr}(\Sigma^{-1} \Gamma) + \alpha \cdot \sqrt{2 \cdot \operatorname{Tr}[(\Sigma^{-1} \Gamma)^2]}) \leq \frac{1}{1 + \alpha^2}. \quad (15)$$

*Proof.* Let us define  $Z := \Sigma^{-1/2}(\mu_x - \bar{\mu}) \sim \mathcal{N}(0, \Lambda)$ , where  $\Lambda := \Sigma^{-1/2} \Gamma \Sigma^{-1/2}$ . Then we can write  $X = Z^\top Z = \|Z\|^2 \sim \sum_{i=1}^d \lambda_i Z_i^2$ , where  $\{Z_i\}_{i=1}^d$  are i.i.d. standard normal variables, and  $\{\lambda_i\}_{i=1}^d$  are the eigenvalues of  $\Lambda$ . Hence,  $X$  is a generalized chi-squared random variable. We now compute its mean and variance,  $\mathbb{E}[X] = \sum_{i=1}^d \lambda_i = \operatorname{Tr}(\Lambda) = \operatorname{Tr}(\Sigma^{-1} \Gamma)$ ,

$$\operatorname{Var}(X) = \sum_{i=1}^d \lambda_i^2 \cdot \operatorname{Var}(Z_i^2) = 2 \sum_{i=1}^d \lambda_i^2 = 2 \cdot \operatorname{Tr}[(\Sigma^{-1} \Gamma)^2].$$

To establish the exponential tail bound, we invoke the Hanson-Wright inequality for quadratic forms of sub-Gaussian vectors (see, e.g., [30]). For a symmetric matrix  $A$  and  $Z \sim \mathcal{N}(0, I)$ , the Hanson-Wright bound gives

$$\mathbb{P}(Z^\top A Z - \mathbb{E}[Z^\top A Z] \geq t) \leq \exp \left( -\frac{t^2}{8 \|A\|_F^2} \right),$$

for all  $t \geq 0$ , where  $\|A\|_F^2 = \operatorname{Tr}(A^2)$ . Applying this with  $A = \Lambda$ , we obtain

$$\mathbb{P}(X \geq \operatorname{Tr}(\Sigma^{-1} \Gamma) + t) \leq \exp \left( -\frac{t^2}{8 \cdot \operatorname{Tr}[(\Sigma^{-1} \Gamma)^2]} \right),$$

which proves the first inequality. For the Cantelli-type bound, we apply the classical one-sided Cantelli inequality [31]

$$\mathbb{P}(X \geq \mathbb{E}[X] + \alpha \cdot \sqrt{\operatorname{Var}(X)}) \leq \frac{1}{1 + \alpha^2},$$

which yields the result.  $\square$

**Corollary 4** (Wasserstein analog of Corollary 3). The squared 2-Wasserstein distance  $X := W_2^2(p_x, \bar{p}) = \|\mu_x - \bar{\mu}\|^2$  satisfies the concentration inequality

$$\mathbb{P}(X \geq \operatorname{Tr}(\Gamma) + t) \leq \exp \left( -\frac{t^2}{8 \operatorname{Tr}(\Gamma^2)} \right), \quad (16)$$

and the one-sided Cantelli-type bound

$$\mathbb{P}(X \geq \operatorname{Tr}(\Gamma) + \alpha \sqrt{2 \operatorname{Tr}(\Gamma^2)}) \leq \frac{1}{1 + \alpha^2}. \quad (17)$$

*Proof.* Let  $\mu_x \sim \mathcal{N}(\bar{\mu}, \Gamma)$ . Define  $Z := \mu_x - \bar{\mu} \sim \mathcal{N}(0, \Gamma)$ , so that  $X = \|Z\|^2$ . Let  $\lambda_1, \dots, \lambda_d$  denote the eigenvalues of  $\Gamma$ . Then we can write  $X = \|Z\|^2 = \sum_{i=1}^d \lambda_i Z_i^2$ , where  $Z_i \sim \mathcal{N}(0, 1)$  are i.i.d. standard normal variables. Thus,  $X$  is a generalized chi-squared random variable. The mean and the variance of the same is calculated as  $\mathbb{E}[X] = \sum_{i=1}^d \lambda_i = \operatorname{Tr}(\Gamma)$ , and  $\operatorname{Var}(X) = 2 \sum_{i=1}^d \lambda_i^2 = 2 \operatorname{Tr}(\Gamma^2)$ , respectively.

Similar to the previous result, to establish the exponential tail bound, we invoke the Hanson-Wright inequality for sub-

Gaussian quadratic forms. For a positive semidefinite matrix  $\Gamma$  and  $Z \sim \mathcal{N}(0, I)$ , it yields

$$\mathbb{P}(Z^\top \Gamma Z \geq \text{Tr}(\Gamma) + t) \leq \exp\left(-\frac{t^2}{8 \text{Tr}(\Gamma^2)}\right),$$

which proves equation (16). Then, for the Cantelli-type bound, we apply the classical inequality

$$\mathbb{P}(X \geq \mathbb{E}[X] + \alpha \cdot \sqrt{\text{Var}(X)}) \leq \frac{1}{1 + \alpha^2},$$

which gives equation (17), completing the proof.  $\square$

More importantly, we study the convergence and fluctuations of the empirical Fréchet mean computed over a growing observation window  $B_R = [-R, R]^2$ . Recall the empirical Fréchet mean over  $B_R$  as  $\hat{p}_R = \mathcal{N}(\hat{\mu}_R, \Sigma)$ , where

$$\hat{\mu}_R := \frac{1}{N_R} \sum_{x \in \Phi \cap B_R} \mu_x, \quad N_R := |\Phi \cap B_R|. \quad (18)$$

**Theorem 3** (Concentration of the empirical Fréchet mean under fixed covariance). *Let us assume that the covariance  $\Sigma \in \mathbb{S}_{++}^d$  is fixed across all  $x \in \Phi$  and that the means  $\mu_x \in \mathbb{R}^d$  are i.i.d. random vectors with  $\mathbb{E}[\mu_x] = \bar{\mu}$ ,  $\text{Cov}(\mu_x) = \Gamma$ , and finite second moments. Then as  $R \rightarrow \infty$ , the empirical mean  $\hat{\mu}_R := \frac{1}{N_R} \sum_{x \in \Phi \cap B_R} \mu_x$  converges in probability to the population mean  $\bar{\mu}$ , and satisfies the asymptotic normality, i.e.,  $\sqrt{N_R}(\hat{\mu}_R - \bar{\mu}) \xrightarrow{d} \mathcal{N}(0, \Gamma)$ , where  $N_R := |\Phi \cap B_R| \sim \text{Poisson}(\lambda|B_R|)$ . Furthermore, the mean squared error satisfies*

$$\mathbb{E}[\|\hat{\mu}_R - \bar{\mu}\|^2] = \mathbb{E}\left[\frac{1}{N_R}\right] \cdot \text{Tr}(\Gamma) \leq \frac{\text{Tr}(\Gamma)}{\lambda|B_R|},$$

and hence decays at the rate  $\mathcal{O}(1/|B_R|)$ .

**Remark.** Under the fixed covariance assumption, the Fréchet mean under both Fisher–Rao and 2-Wasserstein metrics depends only on the mean parameters  $\mu_x$ , and coincides with the Euclidean (or Mahalanobis) average. Therefore, the statistical behavior of  $\hat{p}_R$  is governed entirely by that of  $\hat{\mu}_R$ , making the result applicable to both geometries.

*Proof.* Conditioned on  $N_R = n$ , the  $n$  locations  $\{x_i\}_{i=1}^n$  in  $\Phi \cap B_R$  are uniformly distributed in  $B_R$ . The associated means  $\{\mu_{x_i}\}$  are independent (though not identically distributed), each with finite second moment. The empirical mean  $\hat{\mu}_R = \frac{1}{n} \sum_{i=1}^n \mu_{x_i}$  thus satisfies the Lindeberg-Feller central limit theorem (CLT) for triangular arrays [32], yielding

$$\sqrt{n}(\hat{\mu}_R - \bar{\mu}_n) \xrightarrow{d} \mathcal{N}(0, \Gamma_n),$$

where  $\bar{\mu}_n$  and  $\Gamma_n$  are the empirical spatial averages of  $\mathbb{E}[\mu_x]$  and  $\text{Cov}(\mu_x)$  over the sampled points. As  $n \rightarrow \infty$  (i.e., as  $R \rightarrow \infty$ ), the law of large numbers for the PPP implies that  $\bar{\mu}_n \rightarrow \bar{\mu}$  and  $\Gamma_n \rightarrow \bar{\Gamma}$ . Unconditioning over the Poisson distribution of  $N_R$  and using Slutsky's theorem completes the convergence in distribution [33]. For the second moment, we apply the law of total variance:

$$\mathbb{E}[\|\hat{\mu}_R - \bar{\mu}\|^2] = \mathbb{E}[\text{Tr}(\text{Cov}(\hat{\mu}_R | \Phi))] \leq \mathbb{E}\left[\frac{1}{N_R} \cdot \text{Tr}(\bar{\Gamma})\right],$$

where we use the fact that  $\mu_x$  are conditionally independent

and bounded in second moment. Finally, using the inequality  $\mathbb{E}[1/N_R] \leq 1/\mathbb{E}[N_R] = 1/(\lambda|B_R|)$  completes the proof.  $\square$

## B. Palm Expectation of Local Deviation

We now quantify the average deviation of a randomly chosen node from the global Fréchet mean. Throughout this section the superscript ' $\cdot$ ' denotes the operation under the reduced Palm perspective, i.e., conditioning on the existence of a point of the point process at a given location and then removing it [6].

**Theorem 4** (Deviation of the empirical estimate from the global mean). *Let  $\hat{p}_R^!$  denote the empirical Fréchet mean computed over the region  $B_R \subset \mathbb{R}^d$  under the Palm distribution. Then, under the following regularity conditions:*

- the covariance matrix  $\Sigma \in \mathbb{S}_{++}^d$  is fixed across all  $x \in \Phi$ ,
- the means  $\mu_x \in \mathbb{R}^d$  are i.i.d. with finite second moments,
- the squared geodesic distance  $d^2(p, q)$  on the manifold of Gaussians is locally strongly convex around the Fréchet mean.

there exists a constant  $C > 0$ , independent of  $R$ , such that

$$\mathbb{E}^! [d^2(\hat{p}_R^!, \bar{p})] \leq \frac{C}{\lambda|B_R|},$$

where  $\mathbb{E}^![\cdot]$  denotes expectation under the (reduced) Palm distribution and  $|\cdot|$  denotes Lebesgue measure. This result holds for both Fisher–Rao and 2-Wasserstein metrics when the covariance is fixed. In both cases, the empirical Fréchet mean depends only on the mean parameters  $\mu_x$ , and the squared distance functions are locally convex around the mean. The deviation bound captures the convergence rate of geometry-aware estimators in spatial inference problems.

*Proof:* Let  $\mathcal{M}$  denote the statistical manifold of Gaussian distributions and define the Fréchet functional [14]

$$F(p) := \int_{\mathbb{R}^d} d^2(p_x, p) d\Phi(x),$$

whose minimizer is the global Fréchet mean  $\bar{p} \in \mathcal{M}$ . The empirical Fréchet mean over the ball  $B_R$  under the Palm distribution is  $\hat{p}_R^! := \arg \min_{p \in \mathcal{M}} \sum_{x \in \Phi \cap B_R} d^2(p_x, p)$ , where  $\Phi$  is conditioned to contain a typical point at the origin. Using Campbell's formula under the Palm distribution,

$$\mathbb{E}^![f(\hat{p}_R^!)] = \frac{1}{\lambda|B_R|} \mathbb{E} \left[ \sum_{x \in \Phi \cap B_R} f(\hat{p}_R^{(x)}) \right],$$

where  $\hat{p}_R^{(x)}$  denotes the empirical Fréchet mean when a point is added at location  $x$ . For small perturbations of the Fréchet functional, the deviation can be approximated via a second-order Taylor expansion [34]

$$F(\hat{p}_R^!) - F(\bar{p}) \geq \frac{\kappa}{2} d^2(\hat{p}_R^!, \bar{p}),$$

for some local strong convexity constant  $\kappa > 0$  (ensured by local convexity of the squared geodesic distance on  $\mathcal{M}$ ). Conversely, smoothness implies

$$F(\hat{p}_R^!) - F(\bar{p}) \leq \sup_{p \in \mathcal{M}} \|\nabla F(p)\| \cdot d(\hat{p}_R^!, \bar{p}).$$

Combining the above yields  $d^2(\hat{p}_R^1, \bar{p}) \leq \frac{2}{\kappa} (F(\hat{p}_R^1) - F(\bar{p}))$ . Taking expectations under the Palm distribution and invoking concentration properties of empirical Fréchet functionals over Poisson processes (e.g., from sub-Gaussianity of the squared geodesic distances and independence of marks), we obtain

$$\mathbb{E}^1 [d^2(\hat{p}_R^1, \bar{p})] \leq \frac{2}{\kappa} \mathbb{E}^1 [F(\hat{p}_R^1) - F(\bar{p})] = \mathcal{O} \left( \frac{1}{\lambda |B_R|} \right).$$

The constant  $C$  depends on the curvature of the statistical manifold, the Lipschitz constants of the geodesic distance, and higher moments of the mark distributions  $p_x$ . ■

**Corollary 5** (Variance of the Palm deviation). *Under the assumptions of Theorem 4, there exists a constant  $C' > 0$ , depending only on the curvature and smoothness of the statistical manifold  $\mathcal{M}$ , such that the variance of the geodesic deviation under the Palm distribution satisfies*

$$\text{Var}^1 [d^2(\hat{p}_R^1, \bar{p})] \leq \frac{C'}{(\lambda |B_R|)^2}.$$

*Proof:* Define the random variable  $Z := d^2(\hat{p}_R^1, \bar{p})$ . From Theorem 4, we know  $\mathbb{E}^1[Z] = \mathcal{O}(1/\lambda |B_R|)$ . To bound the variance, we see that

$$\text{Var}^1[Z] = \mathbb{E}^1[Z^2] - (\mathbb{E}^1[Z])^2.$$

Let  $F(p) := \sum_{x \in \Phi \cap B_R} d^2(p_x, p)$  be the empirical Fréchet functional under Palm conditioning. Since  $\hat{p}_R^1$  minimizes  $F(p)$ , the value of  $Z = d^2(\hat{p}_R^1, \bar{p})$  inherits the fluctuations of  $F(\hat{p}_R^1)$  around its expectation. As  $d^2(p_x, \cdot)$  is assumed Lipschitz and sub-Gaussian under both Fisher–Rao and Wasserstein metrics, the CLT for Poisson functionals (see e.g., [35]) implies

$$\mathbb{E}^1[Z^2] = \mathcal{O} \left( \frac{1}{(\lambda |B_R|)^2} \right).$$

Since  $(\mathbb{E}^1[Z])^2 = \mathcal{O}(1/(\lambda |B_R|)^2)$ , the result follows. ■

**Theorem 5** (Palm deviation of the typical point from the global mean). *Let  $p_0 = \mathcal{N}(\mu_0, \Sigma)$  be the distribution associated with a typical point under the Palm distribution of  $\Phi$ . Then:*

$$\mathbb{E}[d^2(p_0, \bar{p}) \mid 0 \in \Phi] = \text{Tr}(\Sigma^{-1} \Gamma) \quad (\text{Fisher–Rao}),$$

and

$$\mathbb{E}[W_2^2(p_0, \bar{p}) \mid 0 \in \Phi] = \text{Tr}(\Gamma) \quad (\text{Wasserstein}).$$

*Proof:* We consider the two metrics separately. Under the Fisher–Rao metric, when all distributions share the same covariance matrix  $\Sigma$ , the squared geodesic distance between two Gaussians  $p_1 = \mathcal{N}(\mu_1, \Sigma)$  and  $p_2 = \mathcal{N}(\mu_2, \Sigma)$  reduces to the Mahalanobis distance:

$$d_{\text{FR}}^2(p_1, p_2) = (\mu_1 - \mu_2)^\top \Sigma^{-1} (\mu_1 - \mu_2).$$

Let  $p_0 = \mathcal{N}(\mu_0, \Sigma)$  be the Gaussian distribution associated with a typical point under Palm conditioning, and let  $\bar{p} = \mathcal{N}(\bar{\mu}, \Sigma)$  be the global Fréchet mean. Then,

$$\mathbb{E}[d^2(p_0, \bar{p}) \mid 0 \in \Phi] = \mathbb{E}[(\mu_0 - \bar{\mu})^\top \Sigma^{-1} (\mu_0 - \bar{\mu})].$$

Since  $\mu_0 \sim \mathcal{N}(\bar{\mu}, \Gamma)$  under the Palm distribution, and  $\Sigma^{-1}$  is

constant,

$$\begin{aligned} \mathbb{E}[d^2(p_0, \bar{p}) \mid 0 \in \Phi] &= \mathbb{E}[\text{Tr}(\Sigma^{-1} (\mu_0 - \bar{\mu})(\mu_0 - \bar{\mu})^\top)] \\ &= \text{Tr}(\Sigma^{-1} \Gamma). \end{aligned}$$

Next, for Gaussians  $p_1 = \mathcal{N}(\mu_1, \Sigma)$ ,  $p_2 = \mathcal{N}(\mu_2, \Sigma)$ , the squared 2-Wasserstein distance reduces to the squared Euclidean distance between means  $W_2^2(p_1, p_2) = \|\mu_1 - \mu_2\|^2$ . Thus,

$$\mathbb{E}[W_2^2(p_0, \bar{p}) \mid 0 \in \Phi] = \mathbb{E}[\|\mu_0 - \bar{\mu}\|^2] = \text{Tr}(\Gamma),$$

since  $\mu_0 \sim \mathcal{N}(\bar{\mu}, \Gamma)$ . This concludes the proof. ■

**Remark 3** (Comparison with Palm pointwise deviation). Theorem 5 provides a closed-form expression for the expected squared geodesic distance between a typical distribution  $p_0$  and the global Fréchet mean  $\bar{p}$  under Palm conditioning. Specifically, it quantifies the intrinsic “semantic variance” at a typical point in the network, with the expected squared distance governed by the second-order statistics of the field of means  $\{\mu_x\}$ . In contrast, Theorem 4 bounds the expected squared deviation of the empirical Fréchet mean  $\hat{p}_R^1$  from  $\bar{p}$  when estimated over a finite region  $B_R$  under Palm conditioning. This result reflects the estimation error incurred in distributed aggregation and scales inversely with the sample size  $\lambda |B_R|$ .

Together, the two results play complementary roles: Theorem 5 characterizes the semantic variability of individual nodes, while Theorem 4 quantifies the convergence rate of geometry-aware empirical estimation. In analogy with classical statistics, the former corresponds to the population variance, whereas the latter captures the error of the sample mean estimator under a Riemannian metric.

## V. DISTRIBUTION OF THE CONDITIONAL FRÉCHET MEAN

In spatially distributed inference, the configuration of agents is itself a source of randomness. While the previous section focused on the expected properties of the Fréchet mean over random Gaussian fields, it is also important to study its distributional behavior conditioned on a realization of the point process. This gives rise to what we refer to as the distribution of the conditional Fréchet mean or more formally, the *meta-distribution* of the Fréchet mean. We study it for the special case of homogeneous PPP.

Let  $\phi \subset \mathbb{R}^2$  be a realization of a homogeneous PPP  $\Phi$  of intensity  $\lambda > 0$ , and as before, let each point  $x \in \phi \cap B_R$  be associated with a random Gaussian distribution  $p_x = \mathcal{N}(\mu_x, \Sigma_x)$ . The empirical Fréchet mean conditioned on the realization  $\phi$  of  $\Phi$  over a window  $B_R \subset \mathbb{R}^2$  is  $\hat{p}_R = \arg \min_{q \in \mathcal{G}} \sum_{x \in \phi \cap B_R} d^2(p_x, q)$ . Naturally, due to the conditioning on the realization,  $\hat{p}_R$  is a random variable with its randomness coming from two sources - the spatial configuration  $\Phi$  and the randomness of the Gaussian parameters  $(\mu_x, \Sigma_x)$  associated to each point  $x \in \phi$ . In this construction,  $\hat{\mu}_R$  and  $\hat{\Sigma}_R$  are now conditionally random variables over a finite random set of i.i.d. samples, whose number  $N_R := |\Phi \cap B_R| \sim \text{Poisson}(\lambda |B_R|)$ . We are particularly interested in the conditional mean  $\mathbb{E}[\hat{\mu}_R \mid \Phi]$ , variance  $\text{Var}[\hat{\mu}_R \mid \Phi]$ , and



similarly for  $\hat{\Sigma}_R$ . An exact analytical characterization of the same is challenging and likely intractable. Accordingly, we provide an approximation by invoking CLT.

#### A. Analytical Approximation via Conditional CLT

Conditioned on  $\Phi \cap B_R = \{x_1, \dots, x_n\}$ , and assuming  $\mu_{x_i} \sim \mathcal{N}(\bar{\mu}, \Gamma)$  i.i.d., we have  $\hat{\mu}_R = \frac{1}{n} \sum_{i=1}^n \mu_{x_i}$ , so  $\hat{\mu}_R \mid \Phi \sim \mathcal{N}(\bar{\mu}, \frac{1}{n}\Gamma)$ . Indeed  $\mathbb{E}[\hat{\mu}_R \mid \Phi] = \bar{\mu}$ , and  $\text{Var}[\hat{\mu}_R \mid \Phi] = \frac{1}{|\Phi \cap B_R|} \Gamma$ , and hence the *meta-distribution* of  $\hat{\mu}_R$  (unconditioned) is a mixture of Gaussians,

$$\hat{\mu}_R \sim \int_{\mathbb{N}} \mathcal{N}\left(\bar{\mu}, \frac{1}{n}\Gamma\right) \cdot \mathbb{P}(N_R = n) dn. \quad (19)$$

This leads to a compound distribution whose variance is:

$$\text{Var}[\hat{\mu}_R] = \mathbb{E}_{\Phi} \left[ \frac{1}{N_R} \Gamma \right] = \Gamma \cdot \mathbb{E} \left[ \frac{1}{N_R} \right].$$

Using Poisson statistics, we can compute:

$$\mathbb{E} \left[ \frac{1}{N_R} \right] \approx \frac{1}{\lambda|B_R| - 1}, \quad \text{for large } \lambda|B_R|.$$

#### B. Cantelli-Type Bounds on the Conditional Fréchet Mean

We now derive a concentration bound for the conditional Fréchet mean of Gaussian distributions defined over a PPP, inspired by the Cantelli-type analysis employed in [36] for bounding the conditional false-alarm probability in radar networks. Recall that for a homogeneous PPP  $\Phi \subset \mathbb{R}^2$  with intensity  $\lambda > 0$ , and for i.i.d. local Gaussian means  $\mu_x \sim \mathcal{N}(\bar{\mu}, \Gamma)$ , the empirical Fréchet mean  $\hat{\mu}_R$  over a bounded observation window  $B_R \subset \mathbb{R}^2$  satisfies:

$$\hat{\mu}_R \mid \Phi \sim \mathcal{N}\left(\bar{\mu}, \frac{\Gamma}{N_R}\right), \quad \text{where } N_R = |\Phi \cap B_R|.$$

Define the deviation random variable  $X := \|\hat{\mu}_R - \bar{\mu}\|^2 \mid \Phi$ , which is conditionally distributed as a weighted chi-squared random variable. Its mean and variance, conditioned on  $\Phi$ , are

$$\mathbb{E}[X \mid \Phi] = \frac{\text{Tr}(\Gamma)}{N_R}; \quad \text{Var}[X \mid \Phi] = \frac{2 \cdot \text{Tr}(\Gamma^2)}{N_R^2}.$$

Applying Cantelli's inequality to the random variable  $X$ , we obtain the following upper bound on the tail probability

$$\mathbb{P}(\|\hat{\mu}_R - \bar{\mu}\|^2 \geq t \mid \Phi) \leq \frac{2 \cdot \text{Tr}(\Gamma^2)/N_R^2}{\left(t - \frac{\text{Tr}(\Gamma)}{N_R}\right)^2 + 2 \cdot \text{Tr}(\Gamma^2)/N_R^2},$$

$$\text{for } t \geq \frac{\text{Tr}(\Gamma)}{N_R}. \quad (20)$$

**Remark 4.** To obtain an unconditional (meta-distributional) bound, we approximate  $N_R \sim \text{Poisson}(\lambda|B_R|)$  using its mean, replacing  $N_R$  by  $\lambda|B_R|$ :

$$\mathbb{P}(\|\hat{\mu}_R - \bar{\mu}\|^2 \geq t) \lesssim \frac{2 \cdot \text{Tr}(\Gamma^2)}{(\lambda|B_R|)^2 \left[ \left(t - \frac{\text{Tr}(\Gamma)}{\lambda|B_R|}\right)^2 + \frac{2 \cdot \text{Tr}(\Gamma^2)}{(\lambda|B_R|)^2} \right]}. \quad (21)$$

This bound captures the tail behavior of the conditional Fréchet mean over spatially distributed agents, offering a

finite-sample confidence guarantee that complements the asymptotic concentration results of the previous section.

**Remark 5.** Compared to (20) which characterizes the tail of the conditional Fréchet mean  $\hat{\mu}_R$ , Corollaries 3 and 4 addresses the distribution of the squared distance  $d^2(p_x, \bar{p})$  between a typical node and the global mean. While both quantities depend on the same Gaussian parameters  $(\bar{\mu}, \Gamma, \Sigma)$ , the above bound captures fluctuations of the empirical mean, whereas the present bound captures fluctuations of an individual agent's deviation. Together, these results provide a comprehensive probabilistic characterization of both global and local deviations in distributed information geometry.

## VI. APPLICATIONS TO WIRELESS SENSOR NETWORKS

Wireless sensor networks are composed of spatially dispersed sensing nodes that collect, process, and transmit information about an environment. In most real-world deployments, the sensor locations are random due to mobility, deployment uncertainty (e.g., aerial drops), or energy-aware reconfiguration. This spatial randomness is well-modeled by a PPP. At the same time, sensors typically produce probabilistic observations-either due to noise, partial observability, or learning-based estimation making the space of observations best described as a manifold of probability distributions. Here, we explore how the framework derived previously for modeling uncertainty in the data provides new analytical tools to quantify and optimize the behavior of WSNs.

Traditionally, WSN analysis assumes a fixed or grid-based topology, scalar measurements aggregated via arithmetic means, and no global geometric structure on sensor beliefs. These assumptions miss critical features such as the case when the nodes may form different local models due to sensing variations. Additionally, sensing quality may vary with location (e.g., terrain or interference). Finally, averages over distributions require respecting the manifold structure (e.g., Fréchet mean over Gaussians as considered in this paper). In particular, for the Gaussian observations, instead of averaging  $\mu_x$  and  $\Sigma_x$  independently, our framework ensures that the aggregation respects the non-Euclidean geometry of the space of distributions. Furthermore, using Palm theory, the expected deviation of a typical node's belief from the global estimate can be quantified as  $\mathbb{E}[W_2^2(p_0, \bar{p}) \mid 0 \in \Phi] = \mathbb{E}[\|\mu_0 - \bar{\mu}\|^2] + \text{covariance mismatch}$ , allowing the network designer to predict confidence mismatches. Finally, our derived results on concentration guarantee that the empirical Fréchet mean  $\hat{p}_R$  over  $B_R$  converges in distribution to  $\bar{p}$ , with variance decaying as  $\sim 1/(\lambda|B_R|)$ . This informs how large a region is required to ensure a specified estimation accuracy.

#### A. Simulation Setup and Results

We consider a wireless sensor network in which each node maintains a Gaussian belief over an unknown global parameter  $\theta \in \mathbb{R}^2$ . The local belief at node  $i$  is modeled as a Gaussian distribution  $\mathcal{N}(\mu_i, \Sigma_i)$ , where  $\mu_i \in \mathbb{R}^2$  is the local mean and  $\Sigma_i \in \mathbb{R}^{2 \times 2}$  is a symmetric positive definite covariance matrix representing uncertainty. To demonstrate the efficacy of

Fréchet averaging under Wasserstein geometry, we simulate a heteroscedastic environment populated with both reliable and unreliable agents. Specifically, 70% of the nodes are designated as reliable, with beliefs  $\mathcal{N}(\mu_i, \Sigma_i)$  where  $\Sigma_i = 0.1 \cdot \mathbf{I}_2$  and  $\mu_i \sim \mathcal{N}(0, \Sigma_i)$ . The remaining 30% are designated as unreliable agents, with beliefs having large covariance  $\Sigma_i = 10 \cdot \mathbf{I}_2$  and strongly biased means  $\mu_i \sim \mathcal{N}([5, 5]^T, \Sigma_i)$ . This models a realistic setting with structured noise due to sensor miscalibration or adversarial corruption.

Sensor locations are drawn from a homogeneous PPP of intensity  $\lambda = 0.1$  over square domains of side length  $2R$ , for  $R \in \{5, 10, 15, 20\}$ . For each realization, two aggregation strategies are compared: (i) Euclidean averaging: The global estimate is computed as  $\hat{\theta}_{\text{Euclid}} = \frac{1}{N} \sum_i \mu_i$ , which disregards the uncertainty in local beliefs; and (ii) Fréchet averaging under the Wasserstein metric: The global estimate is computed as the 2-Wasserstein Fréchet mean of the Gaussian beliefs. The Fréchet mean over Gaussians corresponds to the precision-weighted mean

$$\hat{\theta}_{\text{Fréchet}} = \left( \sum_{i=1}^N \Sigma_i^{-1} \right)^{-1} \left( \sum_{i=1}^N \Sigma_i^{-1} \mu_i \right), \quad (22)$$

which inherently downweights high-variance agents. The performance metric is the mean squared error (MSE) of the global estimate with respect to the ground truth  $\theta = 0$ , averaged over 500 Monte Carlo trials for each value of  $R$ .

Fig. 2 shows the results on a logarithmic scale. We observe that the Euclidean mean suffers from consistently high MSE across all domain sizes due to its inability to suppress the influence of biased, noisy agents. In contrast, the Fréchet mean exhibits substantial error decay as  $R$  increases, since larger deployment regions yield more reliable agents whose precise beliefs dominate the weighted average. These results align with the error scaling predicted in our framework and illustrate the robustness properties of geometry-aware aggregation.

**Remark 6** (System design insight). From a network design perspective, our results state that in order to achieve estimation error below threshold  $\epsilon$ , a network planner must choose region size  $|B_R|$  satisfying

$$\frac{\text{Tr}(\Gamma)}{\lambda |B_R|} \leq \epsilon.$$

## VII. APPLICATIONS TO SEMANTIC COMMUNICATIONS OVER SPATIAL NETWORKS

Semantic communication seeks to transmit information that preserves meaning rather than raw data. In the context of spatially deployed sensor networks, where each agent observes a local phenomenon and encodes its belief as a Gaussian distribution  $p_x = \mathcal{N}(\mu_x, \Sigma_x)$ , it is often inefficient to transmit all sensed data due to bandwidth constraints. Instead, a key objective is to identify a compressed representation that is semantically equivalent in terms of the aggregated global information. To this end, we propose a semantic matching mechanism wherein a dense field of probabilistic beliefs, arising from a high-density PPP, can be approximated by a sparser field whose Fréchet mean is geometrically close under either the Fisher–Rao or 2-Wasserstein distance. This

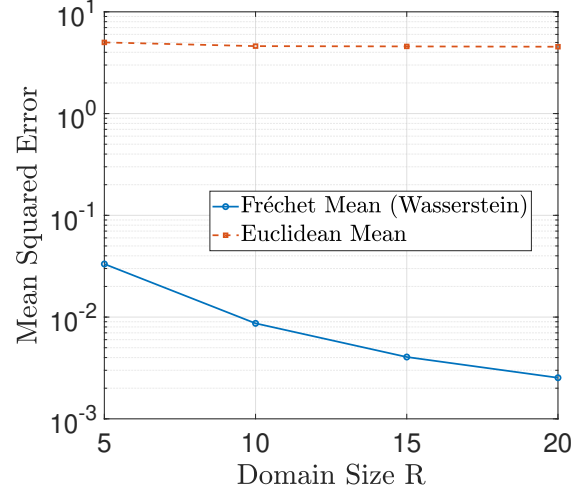


Fig. 2. Comparison of Euclidean and Fréchet (Wasserstein) averaging for heteroscedastic sensor beliefs. The Fréchet mean downweights unreliable agents and exhibits significantly lower MSE.

enables a principled method to compress the sensed process for transmission, while preserving semantic fidelity.

Let  $\Phi$  and  $\Phi'$  be two independent realizations of PPP with intensities  $\lambda \gg \lambda'$ , respectively. The dense process  $\Phi$  models the full sensor field, while  $\Phi'$  represents a compressed or subsampled version. At each location  $x \in \Phi$ , a Gaussian belief  $p_x = \mathcal{N}(\mu_x, \Sigma_x)$  is associated, forming a distribution-valued marked point process. Let  $p_B^{\text{dense}} = \arg \min_{q \in \mathcal{G}} \sum_{x \in \Phi \cap B} d^2(p_x, q)$  and  $p_B^{\text{sparse}} = \arg \min_{q \in \mathcal{G}} \sum_{x \in \Phi' \cap B} d^2(p_x, q)$  denote the empirical Fréchet means over a bounded region  $B \subset \mathbb{R}^2$ , computed under a chosen metric  $d(\cdot, \cdot)$  (Fisher–Rao or Wasserstein). Define the semantic distortion as

$$D(B) := d^2(p_B^{\text{dense}}, p_B^{\text{sparse}}). \quad (23)$$

A sufficient condition for semantic compression is that  $D(B) \leq \epsilon$  for some threshold  $\epsilon > 0$ . This ensures that the sparser process  $\Phi'$  captures the essential semantic content of the original dense field  $\Phi$ .

The empirical Fréchet mean over a PPP with fixed second-order statistics converges to the true global mean, with a mean squared error decaying as  $O(1/\lambda|B|)$ . Assuming both  $\Phi$  and  $\Phi'$  sample from the same distributional field where  $\mu_x \sim \mathcal{N}(\bar{\mu}, \Gamma)$  and  $\Sigma_x = \Sigma$  is fixed, the expected distortion is given by

$$\mathbb{E}[D(B)] \leq \text{Tr}(\Gamma) \left( \frac{1}{\lambda|B|} + \frac{1}{\lambda'|B|} \right). \quad (24)$$

Thus, for a given semantic distortion threshold  $\epsilon$ , the minimum intensity  $\lambda'$  of the sparse process that preserves semantic equivalence satisfies

$$\lambda' \geq \frac{1}{|B|} \cdot \frac{\text{Tr}(\Gamma)}{\epsilon - \text{Tr}(\Gamma)/(\lambda|B|)}. \quad (25)$$

### A. Semantic Communication Protocol

The above analysis yields a practical protocol for semantic communication. First, each node computes a local belief  $p_x = \mathcal{N}(\mu_x, \Sigma_x)$  from its observations. Next, a sparse subset of nodes  $\Phi' \subset \Phi$  is selected such that the Fréchet mean over  $\Phi'$  lies within an  $\varepsilon$ -ball of that over  $\Phi$ . Only these selected nodes transmit their compressed representation  $(\mu_x, \Sigma_x)$  to a central fusion center. This enables effective aggregation without requiring access to all raw observations or dense data streams, thereby saving communication overhead while maintaining global inference accuracy.

### B. Extension to Change Detection and Implications for Network Design

Given two sensor networks  $\Phi_1$  and  $\Phi_2$  with associated Gaussian belief fields  $\{p_x^{(1)}\}$  and  $\{p_x^{(2)}\}$  respectively, we define the semantic similarity as

$$S(\Phi_1, \Phi_2) := d^2(\hat{p}_1, \hat{p}_2), \quad (26)$$

where  $\hat{p}_i$  denotes the empirical Fréchet mean over  $\Phi_i$ . This quantity quantifies the difference in information between two sensed fields and can be used for change detection, spatial clustering of sensor environments, or selection of representative nodes. The results derived herein provide concrete guidelines for the design of semantically efficient communication protocols. For instance, given a distortion constraint  $\varepsilon$  and sensor field intensity  $\lambda$ , one can compute the required density  $\lambda'$  of compressed transmissions. Furthermore, due to the down-weighting of high-variance beliefs in Fréchet averaging (as shown in Section VII), the proposed method is robust to sensor unreliability and supports confidence-weighted information fusion. This leads to improved scalability, energy efficiency, and semantic fidelity in large-scale distributed networks.

## VIII. APPLICATIONS TO MULTI-ARMED BANDITS WITH DISTRIBUTIONAL AND GEOMETRIC STRUCTURE

### A. Motivation

In many modern networked systems, such as wireless sensor networks or edge AI deployments, the reward associated with each decision is naturally modeled as a distribution rather than a scalar. For example, sensors deployed in a spatial domain may report local Gaussian beliefs over an environmental variable, with both the mean and variance depending on local noise conditions and sensing reliability. The spatial locations of these sensors may be random due to deployment uncertainty or mobility, making PPP a realistic model for their distribution. In such settings, selecting which sensor to query at each time step corresponds to a bandit arm with a distributional reward, and exploiting spatial regularity and geometric proximity among arms becomes essential. The Fréchet-UCB algorithm directly models this by combining uncertainty-aware geometric averaging with neighborhood-based exploration, enabling efficient and principled decision-making in spatially embedded, distributionally heterogeneous environments.

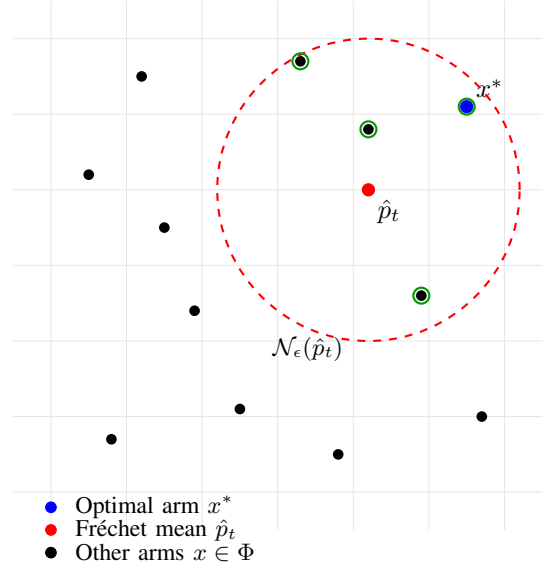


Fig. 3. Spatial geometry of arms under distributional geometric bandits. Arms within the  $\varepsilon$ -neighborhood of the current Fréchet mean are considered for sampling.

### B. MAB Setting

In classical stochastic MAB, each arm  $i \in \{1, \dots, K\}$  yields i.i.d. scalar rewards drawn from an unknown distribution. The learner aims to sequentially select arms to maximize cumulative reward or minimize regret. However, in many modern applications such as recommendation systems, adaptive sensing, and wireless networks the reward of an arm is more naturally described by a probability distribution (e.g., a Gaussian belief over latent states), and the arms may be embedded in a structured space, such as a spatial or semantic manifold. We extend our stochastic-information geometry framework to such distributional geometric bandits (DGB), where the arms correspond to points in a spatial PPP  $\Phi \subset \mathbb{R}^2$ . Each arm  $x \in \Phi$  yields reward  $r_x \sim p_x = \mathcal{N}(\mu_x, \Sigma_x)$ , where  $\mu_x \in \mathbb{R}$  is the mean reward, and  $\Sigma_x \in \mathbb{R}^{1 \times 1}$  represents uncertainty. The learner only has access to sampled rewards from selected arms. Define the optimal arm:

$$x^* := \arg \max_{x \in \Phi} \mu_x.$$

At each time  $t = 1, \dots, T$ , the learner selects  $x_t \in \Phi$ , observes a sample  $r_t \sim p_{x_t}$ , and aims to minimize the cumulative expected regret:

$$\text{Regret}(T) = \mathbb{E} \left[ \sum_{t=1}^T (\mu_{x^*} - \mu_{x_t}) \right].$$

### C. Geometry-Aware Policy via Fréchet Mean

To exploit geometric structure, we maintain an empirical Fréchet mean  $\hat{p}_t$  over the reward distributions of previously sampled arms:

$$\hat{p}_t = \arg \min_{q \in \mathcal{G}} \frac{1}{t} \sum_{s=1}^t d^2(p_{x_s}, q),$$

where  $d(\cdot, \cdot)$  is either the Fisher–Rao or 2-Wasserstein distance on Gaussians. At each time step, the learner chooses an arm  $x \in \Phi$  that minimizes  $x_t = \arg \min_{x \in \mathcal{N}_\epsilon(\hat{p}_t)} \{d^2(p_x, \hat{p}_t) - \beta_t \cdot \text{UCB}_x(t)\}$ , where  $\mathcal{N}_\epsilon(\hat{p}_t) := \{x \in \Phi : d(p_x, \hat{p}_t) \leq \epsilon\}$  is a neighborhood of the current belief,  $\text{UCB}_x(t)$  is an exploration term, e.g., proportional to  $\sqrt{\log t / n_x(t)}$ , and  $\beta_t$  is a tunable exploration parameter.

The rationale behind selecting the arm that minimizes the geodesic distance to the empirical Fréchet mean augmented with an upper confidence bound stems from the distributional and geometric structure of the reward space. Unlike classical bandit problems, where each arm yields a scalar reward, in our setting each arm corresponds to a Gaussian distribution  $p_x = \mathcal{N}(\mu_x, \Sigma_x)$ , thereby residing on a statistical manifold endowed with either the Fisher–Rao or 2-Wasserstein geometry. The empirical Fréchet mean  $\hat{p}_t$  at time  $t$  serves as a geometry-aware aggregate of the previously sampled arms’ reward distributions. As such, it encapsulates both central tendency and uncertainty in a manner that is consistent with the manifold structure.

By minimizing the squared geodesic distance  $d^2(p_x, \hat{p}_t)$  over a neighborhood  $\mathcal{N}_\epsilon(\hat{p}_t)$ , the algorithm restricts exploration to arms whose distributions are geometrically close to the current aggregate belief. This locality constraint effectively reduces unnecessary exploration of arms whose reward distributions are far from the high-reward region, as determined by the learned geometry. To incorporate exploration, an upper confidence bonus  $\text{UCB}_x(t)$ , typically of the form  $\sqrt{2 \log t / n_x(t)}$ , is subtracted from the distance term, scaled by a tunable parameter  $\beta_t$ . The resulting acquisition rule,

$$x_t = \arg \min_{x \in \mathcal{N}_\epsilon(\hat{p}_t)} \{d^2(p_x, \hat{p}_t) - \beta_t \cdot \text{UCB}_x(t)\},$$

therefore balances exploitation of arms that are geometrically aligned with past observations and exploration of uncertain arms within this trusted region.

#### D. Proposed Algorithm: FRÉCHET-UCB

---

##### Algorithm 1 FRÉCHET-UCB BANDIT ALGORITHM

---

- 1: Initialize:  $S_0 \leftarrow \emptyset$ ,  $\hat{p}_0 \leftarrow$  arbitrary prior
- 2: **for** each round  $t = 1, \dots, T$  **do**
- 3:   Define local neighborhood  $\mathcal{N}_\epsilon(\hat{p}_{t-1}) \subset \Phi$
- 4:   **for** each  $x \in \mathcal{N}_\epsilon$  **do**
- 5:     Compute empirical mean  $\hat{\mu}_x(t)$ , count  $n_x(t)$
- 6:     Compute UCB:  $\text{UCB}_x(t) = \hat{\mu}_x(t) + \sqrt{2 \log t / n_x(t)}$
- 7:   **end for**
- 8:   Select arm:

$$x_t = \arg \min_{x \in \mathcal{N}_\epsilon(\hat{p}_t)} \{d^2(p_x, \hat{p}_t) - \beta_t \cdot \text{UCB}_x(t)\}$$

- 9:   Sample reward  $r_t \sim p_{x_t}$ , update posterior for  $p_{x_t}$
  - 10:   Update empirical Fréchet mean  $\hat{p}_t$  using  $\{p_{x_s}\}_{s=1}^t$
  - 11: **end for**
- 

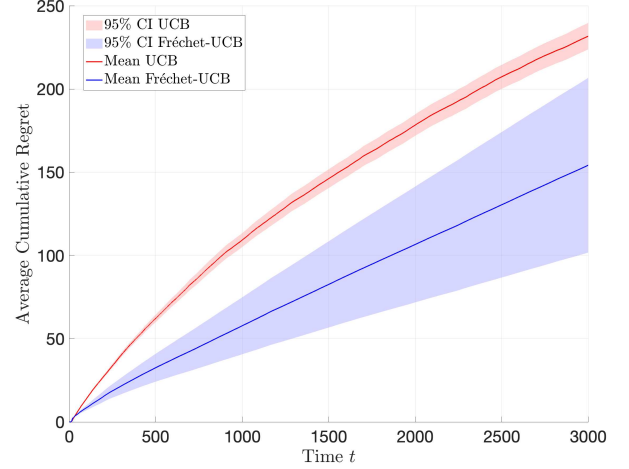


Fig. 4. Comparison of average cumulative regret for classical UCB and Fréchet-UCB over 100 trials in a heteroscedastic bandit setting. Fréchet-UCB outperforms classical UCB by favoring arms that are geometrically consistent with the precision-weighted global belief, effectively avoiding over-exploration of high-variance arms. Shaded regions denote 95% confidence intervals.

#### E. Simulation Setup and Results

To illustrate the performance advantage of Fréchet-UCB over classical UCB, we consider a curated multi-armed bandit environment with  $K = 10$  arms, where each arm yields a Gaussian reward with fixed but unknown mean and variance.

The arms are divided into three groups: Arms 1-3 have high mean ( $\mu \in [0.87, 0.9]$ ) and high variance ( $\sigma^2 = 2.25$ ), Arms 4-7 have moderately high mean ( $\mu \in [0.72, 0.75]$ ) and low variance ( $\sigma^2 = 0.01$ ), while Arms 8-10 have low mean ( $\mu \in [0.4, 0.5]$ ) and low variance. The total horizon is  $T = 3000$ , and results are averaged over 100 independent trials.

The Fréchet-UCB policy maintains a precision-weighted estimate of the global belief, given by the empirical Fréchet mean  $\hat{\mu}_{\text{Fr}}(t) = \sum_k w_k(t) \hat{\mu}_k(t) / \sum_k w_k(t)$ , where  $w_k(t) = 1 / \hat{\sigma}_k^2(t)$ . At each round, it selects the arm maximizing the acquisition function  $d^2(p_x, \hat{p}_t) - \beta_t \cdot \text{UCB}_x(t)$ , where  $\alpha$  and  $\lambda$  are tunable parameters and  $n_k(t)$  is the number of times arm  $k$  has been played. This scoring function naturally balances exploitation, statistical confidence, and geometric consistency with the global belief.

The simulation results are shown in Fig. 4. Fréchet-UCB demonstrates significantly lower cumulative regret than classical UCB, particularly as  $t$  increases. While classical UCB over-explores the high-variance arms due to their high empirical means, Fréchet-UCB correctly downweights these due to their statistical unreliability and instead concentrates sampling on moderately high-mean, low-variance arms that offer consistent returns. The shaded regions show 95% confidence intervals across trials, confirming the statistical significance of the performance gap. These results validate the effectiveness of geometry-aware exploration in structured bandit environments with heteroscedastic reward distributions.

## F. Regret Analysis

Although a complete analysis of the regret of Fréchet UCB is out of scope for this work, we provide a sketch of the proof in this section. Let  $\delta_x := \mu_{x^*} - \mu_x$  denote the suboptimality gap.

**Theorem 6** (Regret Bound for FRÉCHET-UCB). *For the FRÉCHET-UCB policy under mild assumptions on the continuity of  $\mu_x$  in the Wasserstein geometry, and bounded variance  $\sigma_x^2 \leq \sigma_{\max}^2$ , for any neighborhood radius  $\epsilon > 0$ , the cumulative regret up to time  $T$  satisfies*

$$\text{Regret}(T) = \mathcal{O} \left( \sum_{x \in \Phi_\epsilon} \frac{\log T}{\Delta_x} + \lambda |\mathbb{R}^2 \setminus \mathcal{N}_\epsilon| \cdot \Delta_{\max} \cdot T \right),$$

where  $\Phi_\epsilon := \{x \in \Phi : d(p_x, p_{x^*}) \leq \epsilon\}$ ,  $\mathcal{N}_\epsilon := \{x \in \Phi : d(p_x, \hat{p}_t) \leq \epsilon\}$  is the neighborhood used by the algorithm at time  $t$ , and  $\Delta_{\max} := \sup_{x \in \Phi} \Delta_x$ .

*Proof.* The proof follows from decomposing regret into (i) rounds where arms in  $\Phi_\epsilon$  are played, applying classical UCB analysis and (ii) rounds where arms outside  $\Phi_\epsilon$  are played, controlled by concentration of  $\hat{p}_t$  and the geometry-aware shrinking of  $\mathcal{N}_\epsilon$ . Bounding the expected number of suboptimal plays yields the result. First, we decompose the regret as

$$\text{Regret}(T) = \sum_{t=1}^T \mathbb{E}[\mu_{x^*} - \mu_{x_t}] = \sum_{x \in \Phi} \Delta_x \cdot \mathbb{E}[N_x(T)],$$

where  $N_x(T)$  is the number of times arm  $x$  is played up to time  $T$ .

For any suboptimal arm  $x \in \Phi_\epsilon$ , and assuming the UCB estimates are valid (i.e.,  $x \in \mathcal{N}_\epsilon(\hat{p}_t)$ ), classical UCB analysis yields:

$$\mathbb{E}[N_x(T)] \leq \frac{8 \log T}{\Delta_x^2} + 1 + \frac{\pi^2}{3},$$

under sub-Gaussian noise and bounded variance. Hence, the regret contribution from arms in  $\Phi_\epsilon$  is

$$\sum_{x \in \Phi_\epsilon} \Delta_x \cdot \mathbb{E}[N_x(T)] = \mathcal{O} \left( \sum_{x \in \Phi_\epsilon} \frac{\log T}{\Delta_x} \right).$$

Let  $\mathcal{E}_t$  denote the event that the empirical Fréchet mean  $\hat{p}_t$  lies outside the  $\epsilon$ -ball of the true optimal distribution:

$$\mathcal{E}_t := \{d(\hat{p}_t, p_{x^*}) > \epsilon\}.$$

By concentration of the empirical Fréchet mean, there exist constants  $c_1, c_2 > 0$  such that

$$\mathbb{P}[\mathcal{E}_t] \leq c_1 e^{-c_2 \lambda t \epsilon^2}.$$

Let  $\Phi' := \Phi \setminus \Phi_\epsilon$ . Since the algorithm selects arms only in  $\mathcal{N}_\epsilon(\hat{p}_t)$ , arms from  $\Phi'$  can be selected only if  $\mathcal{E}_t$  occurs. Thus:

$$\mathbb{E} \left[ \sum_{t=1}^T \mathbb{1}_{\{x_t \in \Phi'\}} \right] \leq \sum_{t=1}^T \mathbb{P}[\mathcal{E}_t] \cdot |\Phi'|.$$

While this sum is finite due to exponential decay, we conservatively upper bound this component by assuming that in the worst case, any arm in  $\mathbb{R}^2 \setminus \mathcal{N}_\epsilon$  can be chosen during those

steps, leading to:

$$\text{Regret}_{\text{outer}}(T) \leq \lambda |\mathbb{R}^2 \setminus \mathcal{N}_\epsilon| \cdot \Delta_{\max} \cdot T.$$

Combining both components, we obtain:

$$\text{Regret}(T) \leq \mathcal{O} \left( \sum_{x \in \Phi_\epsilon} \frac{\log T}{\Delta_x} \right) + \lambda |\mathbb{R}^2 \setminus \mathcal{N}_\epsilon| \cdot \Delta_{\max} \cdot T.$$

□

## G. Comparison of Fréchet-UCB and Classical UCB

The key difference lies in how the algorithms treat the structure of the reward space. Classical UCB operates under the assumption that each arm yields a real-valued reward drawn i.i.d. from a fixed distribution, and focuses solely on estimating the mean reward. In contrast, Fréchet-UCB operates in a space where each arm yields a full probability distribution (e.g., a Gaussian belief) and distances between arms are computed using a geometry-aware metric, such as the Fisher–Rao distance.

When the reward associated with each arm is not a scalar but a distribution—for example, a Gaussian  $p_x = \mathcal{N}(\mu_x, \sigma_x^2)$ —classical UCB discards important information about uncertainty or belief shape, relying only on the estimated mean  $\mu_x$ . Fréchet-UCB, by contrast, treats the space of distributions as a Riemannian manifold and incorporates both mean and variance information via geodesic distances. This is particularly beneficial in settings where arms are not independent but lie on a structured space, such as a spatial domain or a semantic similarity graph. Moreover, the use of the Fisher–Rao metric provides a natural framework for confidence-aware decision making. For instance, in distributionally robust scenarios where the learner must be sensitive to both central tendency and variability, the Fisher–Rao geometry reflects the curvature of the statistical manifold and provides meaningful distances even when the mean rewards are close.

## IX. CONCLUSION

This paper has introduced a unified framework that bridges stochastic geometry, information geometry, and online decision theory to address the problem of inference and exploration over spatially distributed statistical fields. We developed a rigorous analysis of the empirical Fréchet mean for Gaussian distributions indexed by a PPP, under both the Fisher–Rao and Wasserstein geometries. Leveraging tools from Palm calculus and empirical process theory on manifolds, we established concentration inequalities, meta-distribution characterizations, and convergence rates for geometry-aware aggregation.

Building on this foundation, we proposed the Fréchet-UCB algorithm for bandit problems where each arm yields a Gaussian distribution, and the arm set may be spatially embedded. The algorithm incorporates both local uncertainty and global geometric coherence via a penalized acquisition rule centered around the evolving Fréchet mean. Theoretical regret bounds reveal a two-phase behavior that distinguishes between arms lying within a geodesic neighborhood of the belief and those that are statistically or geometrically inconsistent.

The techniques presented here open several directions for further investigation. On the theoretical front, one may seek sharp non-asymptotic lower bounds on the regret under curvature constraints on the statistical manifold. On the algorithmic side, extensions to non-Gaussian distributions, higher-order information metrics, and adaptive geodesic neighborhoods could further improve sample efficiency. More broadly, this work contributes to an emerging geometric view of learning and inference, where statistical objects are treated as elements of curved spaces, and information-theoretic limits are governed by their intrinsic geometry.

## REFERENCES

- [1] J.-F. Chamberland and V. Veeravalli, “How dense should a sensor network be for detection with correlated observations?” *IEEE Transactions on Information Theory*, vol. 52, no. 11, pp. 5099–5106, 2006.
- [2] T. Liang, T. Poggio, A. Rakhlin, and J. Stokes, “Fisher-rao metric, geometry, and complexity of neural networks,” in *The 22nd international conference on artificial intelligence and statistics*. PMLR, 2019, pp. 888–896.
- [3] H. K. Miyamoto, F. C. Meneghetti, J. Pinele, and S. I. Costa, “On closed-form expressions for the fisher–rao distance,” *Information Geometry*, vol. 7, no. 2, pp. 311–354, 2024.
- [4] J. A. Cuesta and C. Matrán, “Notes on the Wasserstein metric in Hilbert spaces,” *The Annals of Probability*, pp. 1264–1276, 1989.
- [5] T. Lin and H. Zha, “Riemannian manifold learning,” *IEEE transactions on pattern analysis and machine intelligence*, vol. 30, no. 5, pp. 796–809, 2008.
- [6] S. N. Chiu, D. Stoyan, W. S. Kendall, and J. Mecke, *Stochastic geometry and its applications*. John Wiley & Sons, 2013.
- [7] W. Chen, M. R. D. Rodrigues, and I. J. Wassell, “A frechet mean approach for compressive sensing data acquisition and reconstruction in wireless sensor networks,” *IEEE Transactions on Wireless Communications*, vol. 11, no. 10, pp. 3598–3606, 2012.
- [8] S.-i. Amari and H. Nagaoka, *Methods of Information Geometry*. American Mathematical Society, 2007.
- [9] X. Pennec, “Intrinsic statistics on riemannian manifolds: Basic tools for geometric measurements,” *Journal of Mathematical Imaging and Vision*, vol. 25, no. 1, pp. 127–154, 2006.
- [10] H. L. Van Trees and K. L. Bell, *Covariance, Subspace, and Intrinsic CramrRao Bounds*, 2007, pp. 430–450.
- [11] A. Takatsu, “Wasserstein geometry of Gaussian measures,” *Osaka Journal of Mathematics*, vol. 48, no. 4, pp. 1005–1026, 2011.
- [12] L. Malago, A. Monge, and G. Pistone, “Wasserstein Riemannian geometry of Gaussian densities,” *Information Geometry*, vol. 1, no. 2, pp. 137–179, 2018.
- [13] M. Arjovsky, S. Chintala, and L. Bottou, “Wasserstein gan,” in *arXiv:1701.07875*.
- [14] Y. Zemel, “Fréchet means in wasserstein space: theory and algorithms,” Ph.D. dissertation, Ecole Polytechnique Fédérale de Lausanne, 2017.
- [15] M. Haenggi, *Stochastic Geometry for Wireless Networks*. Cambridge University Press, 2012.
- [16] F. Baccelli and B. Błaszczyszyn, *Stochastic Geometry and Wireless Networks: Volume I Theory*. Now Publishers Inc., 2009.
- [17] R. Olfati-Saber, J. A. Fax, and R. M. Murray, “Consensus and cooperation in networked multi-agent systems,” *Proceedings of the IEEE*, vol. 95, no. 1, pp. 215–233, 2007.
- [18] M. Staib, S. Claiici, J. M. Solomon, and S. Jegelka, “Parallel streaming Wasserstein barycenters,” *Advances in Neural Information Processing Systems*, vol. 30, 2017.
- [19] R. Bhatia, *Positive Definite Matrices*. Princeton University Press, 2009.
- [20] I. F. Akyildiz, W. Su, Y. Sankarasubramaniam, and E. Cayirci, “A survey on sensor networks,” *IEEE Communications Magazine*, vol. 40, no. 8, pp. 102–114, 2002.
- [21] D. Russo, B. Van Roy, A. Kazerouni, I. Osband, and Z. Wen, “A tutorial on thompson sampling,” *Foundations and Trends in Machine Learning*, vol. 11, no. 1, pp. 1–96, 2018.
- [22] S. Bubeck and N. Cesa-Bianchi, “Regret analysis of stochastic and nonstochastic multi-armed bandit problems,” *Foundations and Trends in Machine Learning*, vol. 5, no. 1, pp. 1–122, 2012.
- [23] M. Rowland, K. M. Choromanski, F. Chalus, A. Pacchiano, T. Sarlos, R. E. Turner, and A. Weller, “Geometrically coupled monte carlo sampling,” *Advances in Neural Information Processing Systems*, vol. 31, 2018.
- [24] H. Q. Minh, “Fisher–rao geometry of equivalent gaussian measures on infinite-dimensional hilbert spaces,” *Information Geometry*, vol. 7, no. Suppl 2, pp. 781–843, 2024.
- [25] J. Pinele, J. E. Strapasson, and S. I. Costa, “The fisher–rao distance between multivariate normal distributions: Special cases, bounds and applications,” *Entropy*, vol. 22, no. 4, p. 404, 2020.
- [26] S. Bonnabel, “Stochastic gradient descent on riemannian manifolds,” *IEEE Transactions on Automatic Control*, vol. 58, no. 9, pp. 2217–2229, 2013.
- [27] J. Hu, X. Liu, Z.-W. Wen, and Y.-X. Yuan, “A brief introduction to manifold optimization,” *Journal of the Operations Research Society of China*, vol. 8, no. 2, pp. 199–248, 2020.
- [28] G. J. McLachlan, “Mahalanobis distance,” *Resonance*, vol. 4, no. 6, pp. 20–26, 1999.
- [29] A. Anastasiou and R. E. Gaunt, “Wasserstein distance error bounds for the multivariate normal approximation of the maximum likelihood estimator,” *Electronic Journal of Statistics*, vol. 15, no. 2, pp. 5758–5810, 2021.
- [30] M. Rudelson and R. Vershynin, “Hanson-wright inequality and sub-gaussian concentration,” 2013.
- [31] N. Apollonio, “Cantelli’s bounds for generalized tail inequalities,” *Axioms* (2075-1680), vol. 14, no. 1, 2025.
- [32] J. Bethmann, “The lindberg–feller theorem for sums of a random number of independent random variables in a triangular array,” *Theory of Probability & Its Applications*, vol. 33, no. 2, pp. 334–339, 1989.
- [33] F. Delbaen, “A remark on slusky’s theorem,” in *Séminaire de Probabilités XXXII*. Springer, 2006, pp. 313–315.
- [34] B. Dupire and V. Tissot-Daguette, “Functional expansions,” *arXiv preprint arXiv:2212.13628*, 2022.
- [35] M. D. Penrose, “Convergence of random measures in geometric probability,” *arXiv preprint math/0508464*, 2005.
- [36] G. Ghatak, “Distribution bounds on the conditional roc in a poisson field of interferers and clutters,” 2025.